

# Theoretical Modeling of the Feedback Stabilization of External MHD Modes in Toroidal Geometry.<sup>1</sup>

M. S. Chance 1), M. S. Chu 2), M. Okabayashi 1)

1) Princeton Plasma Physics Laboratory, Princeton, NJ

2) General Atomics, San Diego, CA

mchance@pppl.gov

**Abstract.** A theoretical framework for understanding the feedback mechanism against external MHD modes has been formulated. Efficient computational tools – the GATO stability code coupled with a substantially modified VACUUM code – have been developed to effectively design viable feedback systems against these modes. The analysis assumed a thin resistive shell and a feedback coil structure accurately modeled in  $\theta$ , with only a single harmonic variation in  $\phi$ . An optimized configuration and placement of the feedback and sensor coils as well as the time constants and induced currents in the enclosing resistive shell have been computed for the DIII-D device. Up to 90% of the effectiveness of an ideal wall can be achieved.

## 1. Introduction

Unstable external MHD modes are arguably the most important factor inhibiting the progress towards stable advanced toroidal fusion reactor configurations. The presence of a conducting shell surrounding the plasma can only slow the Alfvénic modes to the resistive decay time scale ( $\tau_w$ ) of the shell. The instabilities then manifest themselves as “Resistive Wall Modes” (RWM). They are, however, generally slow enough to allow judicious use of feedback mechanisms to further suppress them in tokamaks [1–4] and reversed field pinches (RFP) [5]. Since reactor grade RWMs cannot be easily stabilized by plasma flow [3, 4, 6], alternative means have become a topic of vital importance. In advanced operation the modes are localized enough at the large major radius side to simplify the spatial requirements of the feedback system [1, 2, 7]. Preliminary experiments showed promising results in temporarily postponing the RWM onset with modest demands from an external feedback coil system [5, 8].

With the inclusion of resistive wall and feedback circuits, the response of the external vacuum region to a given plasma perturbation at the plasma surface is modified from that of a passive vacuum. We present a new formulation of this interaction between the plasma and the vacuum region in general toroidal geometry. In general, in contrast to ideal MHD, the present formulation is non-self-adjoint and includes the necessary pressure balance, but there are idealized cases which retain the self-adjoint property and can be treated by the GATO-VACUUM combination.

---

<sup>1</sup>Work supported by U.S. Department of Energy Contract Nos. DE-AC02-76-CH03073 and DE-AC03-99ER54463.

## 2. The Magnetic Scalar Potential and the Perturbed Pressure

The VACUUM code uses Green's second theorem and the free space Green's function,  $G(\mathbf{r}, \mathbf{r}')$ , to relate the magnetic scalar potential  $\chi$  to the fields of the surfaces. Using  $d\mathbf{S}' = \mathcal{J} \nabla' \mathcal{Z} d\theta' d\phi'$ , where  $\nabla' \mathcal{Z}$  is normal to the vacuum surface in a coordinate system with  $\mathcal{J} = (\nabla \mathcal{Z} \times \nabla \theta \nabla \phi)^{-1}$ , one can write after performing the integration in  $\phi$ ,

$$2\chi(\boldsymbol{\rho}) + \int_C \chi(\theta') \mathcal{K}(\boldsymbol{\rho}, \theta') d\theta' = \int_{C_p + C_w} \mathcal{G}(\boldsymbol{\rho}, \theta') \mathcal{B}(\theta') d\theta', \quad (1)$$

where  $\mathcal{G}(\boldsymbol{\rho}, \theta') = 1/2\pi \oint G(\mathbf{r}, \mathbf{r}') e^{in(\phi - \phi')} d\phi'$ ,  $\mathcal{K}(\boldsymbol{\rho}, \theta') = 1/2\pi \oint \mathcal{J} \nabla' G(\mathbf{r}, \mathbf{r}') \cdot \nabla' \mathcal{Z} e^{in(\phi - \phi')}$  and  $\mathcal{B}(\theta') = \mathcal{J} \nabla' \chi \cdot \nabla' \mathcal{Z}$ . The solution for the plasma response,  $\mathcal{C}^{ss'}$ , on an observer surface  $s$  to the perturbed normal magnetic field  $\mathcal{B}^{s'}$  on each of the source surfaces  $s'$  enclosing the region, expanded in a suitable set of basis functions has the form,

$$\chi^s(\theta_i^s) = \sum_l \mathcal{C}_l^{ss'}(\theta_i^s) \mathcal{B}_l^{s'}. \quad (2)$$

The perturbed vacuum pressure is given by

$$\mathcal{P} \equiv \mathcal{J} \mathbf{B} \cdot \nabla \chi = \psi' \left( \frac{\partial}{\partial \theta} + \frac{\mathbf{B} \cdot \nabla \phi}{\mathbf{B} \cdot \nabla \theta} \frac{\partial}{\partial \phi} \right) \chi. \quad (3)$$

In general the continuity of both  $\mathcal{B}$  and  $\mathcal{P}$  must be satisfied at the interface so Eqs. (2) and (3) give the requisite boundary conditions for stability codes such as MARS, NOVA or DCON. If the feedback problem can utilize the energy principle in its extended form then the continuity of  $\mathcal{P}$  can be ignored. One such instance is described in this study.

## 3. The Feedback Components with a Resistive Shell

The upgraded VACUUM includes the effect of a resistive shell and contributions from feedback coils and sensor loops. The fields on the shell,  $\mathcal{B}^w$ , in Eq. (2) can be eliminated in terms of the perturbation  $\mathcal{B}^p$  at the plasma surface. To this end, a thin shell is assumed with thickness  $\Delta$  and resistivity  $\eta$ , with the field  $\mathcal{B}^w$  assumed continuous and the shell current related to the jump in  $\chi^w$ .  $\mathcal{B}^w$  and the stream function  $\mathcal{I}^w$  of the shell current  $\mathbf{J}^w = \nabla \mathcal{Z} \times \nabla \mathcal{I}^w \delta(\mathcal{Z} - \mathcal{Z}^w)$  are expanded in terms of solutions  $\psi_{l_w}$  of the vessel's surface Laplacian equation obtained from the application of Ampere's and Faraday's laws at the shell:

$$\mathcal{B}^w(\theta) = \sum_{l_w} \mathcal{B}_{l_w}^w \psi_{l_w}(\theta_w), \quad \text{and} \quad \mathcal{I}^w(\theta) = \sum_{l_w} \mathcal{I}_{l_w}^w \psi_{l_w}(\theta_w), \quad (4)$$

where  $\nabla \cdot [\eta(\nabla \mathcal{Z} \times \nabla \psi_{l_w}) \times \nabla \mathcal{Z}] \equiv \nabla_s \cdot \eta \nabla_s \psi_{l_w} = \lambda_{l_w} \psi_{l_w}$  defines the set of expansion eigenvectors and eigenvalues.

Upon coupling to the plasma and the external coils the surface current distribution is found to be determined by a set of coupled time dependent equations. They can be viewed as a set of L/R circuits of the normal magnetic field on the surface  $\tilde{\mathcal{B}}_{l_s}^w$  driven by the plasma perturbations  $\mathcal{B}_{l_p}^p$  and external feedback coils through  $\tilde{I}_{l_s}$ ,

$$\left( \frac{\mu_0 \Delta}{\eta} \frac{\partial}{\partial t} + \tilde{M}_{l_s} \right) \tilde{\mathcal{B}}_{l_s}^w = \sum_{l_p} \tilde{\mathcal{C}}_{l_s l_p}(w, p) \mathcal{B}_{l_p}^p - \mathcal{S} \tilde{I}_{l_s}, \quad (5)$$

where the relation has been transformed to the space where the resistive wall response matrix  $\widetilde{M}_{l_s}$  of the discontinuity of  $\chi$  across the shell is diagonal. The feedback coil component  $\widetilde{I}$  arises from the discontinuity of  $\chi$  in the integral involving  $\mathcal{K}$  of Eq. (1). A choice of  $\widetilde{I}$  modeling the coils of DIII-D is described below. The sensor component of the feedback is given by  $\mathcal{S}$ , which can be composed of contributions multiplied by a gain factor  $G$  from the relevant surfaces, i.e.,  $\mathcal{S} = G^p \sum_{l_p} \mathcal{S}_{l_p}^p \mathcal{B}_{l_p}^p + G^w \sum_{l_s} \mathcal{S}_{l_s}^w \mathcal{B}_{l_s}^w$  if there are sensors located on the plasma and the shell. This can be generalized for loops located away from surfaces by a further application of Green's second identity [7]. This set of equations is equivalent to [9] and reduces to that of [10] in the cylindrical limit.

### 3.1 The Feedback Coil and Sensor Loops

The “window-pane” feedback coil of DIII-D can be modeled accurately in the poloidal angle,  $\theta$ , but only approximately by a single harmonic in  $\phi$ . A divergence-free representation for the current  $\mathbf{J}^c$  is through a current potential  $\mathcal{I}^c(\theta, \phi)$ :  $\mathbf{J}^c = \nabla \mathcal{Z} \times \nabla \mathcal{I}^c \delta(\mathcal{Z} - \mathcal{Z}_c)$ . Then

$$J_\theta^c = -\frac{|\nabla \mathcal{Z}|}{X} \frac{\partial \mathcal{I}^c}{\partial \phi} e^{-in\phi}, \quad \text{and} \quad J_\phi^c = \left( \frac{|\nabla \mathcal{Z}|^2}{X_\theta^2 + Z_\theta^2} \right)^{1/2} \frac{\partial \mathcal{I}^c}{\partial \theta} e^{-in\phi}, \quad (6)$$

suppressing the  $\delta(\mathcal{Z} - \mathcal{Z}_c)$  factor. Here,  $[X(\theta), Z(\theta)]$  parameterizes the “shell” onto which the coil is embedded. A representation for  $\mathcal{I}^c$  for the “window-pane” coils (the C-coils) is given by  $\mathcal{I}^c(\theta, \phi) = \exp[(\cos \theta - \cos \theta_0)/\tau] / \{ \exp[(\cos \theta - \cos \theta_0)/\tau] + 1 \} e^{-in\phi}$ . An example of the current with  $\tau = 0.1$  and width given by  $\theta_0 = \pi/4$  is shown in a  $(\phi-\theta)$  projection in Fig. 1.

If the sensors measure the flux then for loops bounded by  $[(\theta_1, \phi_1), (\theta_2, \phi_2)]$  at the plasma surface, the flux  $\Phi^p$  there is given in terms of a Fourier basis by,

$$\Phi^p = \int_{(\theta_1, \phi_1)}^{(\theta_2, \phi_2)} \mathcal{B}^p(\theta, \phi) d\theta d\phi \equiv \sum_{l_p} \mathcal{B}_{l_p} \Phi_{l_p}^p, \quad (7)$$

where  $\Phi_{l_p}^p = (2/nl_p) \mathcal{P}^p(\phi_1, \phi_2) [\sin l_p(\theta_2 - \theta_1)/2] \exp il_p(\theta_2 - \theta_1)/2$ , and  $\mathcal{P}^p$  has a similar functional form of  $\phi$  as that of the  $\theta$  dependence.

At the resistive shell the the flux through the sensors is similarly decomposed in terms of the eigensolutions  $\psi_{l_s}(\theta)$  of  $\widetilde{M}_{l_s}$ , so  $\Phi_{l_s}^w = i[\mathcal{P}^w(\phi_1, \phi_2)/n] \int_{\theta_1}^{\theta_2} \psi_{l_s}(\theta) d\theta$ .

With the inclusion of these sensor components, Eq. (5) becomes:

$$\sum_{l'_s} \Gamma_{l_s l'_s} \widetilde{\mathcal{B}}_{l'_s}^w = \sum_{l_p} \Xi_{l_s l_p} \mathcal{B}_{l_p}^p, \quad \text{where} \quad (8)$$

$$\Gamma_{l_s l'_s} \equiv \left( \frac{\mu_0 \Delta}{\eta} \frac{\partial}{\partial t} + \widetilde{M}_{l_s} \right) \delta_{l_s l'_s} + G^w \widetilde{I}_{l_s} \Phi_{l'_s}^w, \quad \text{and} \quad \Xi_{l_s l_p} \equiv \left( \widetilde{\mathcal{C}}_{l_s l_p}(w, p) - G^p \widetilde{I}_{l_s} \Phi_{l_p}^p \right).$$

## 4. The Plasma Surface Response

Eq. (8) gives the time dependent relation for the field on the shell in terms of the source plasma perturbation. If we assume  $\partial/\partial t \rightarrow \gamma$  and setting  $\mu_0 \Delta/\eta = \hat{\tau}$  we can invert  $\Gamma$  and solve

explicitly for  $\tilde{\mathcal{B}}_{l'_s}^w$  and use Eq. (2) with  $(ss') \rightarrow (pw)$  to obtain,

$$\chi_{l'_p}^p = \sum_{l_p} \mathcal{B}_{l_p}^p \left[ \mathcal{C}_{l'_p l_p}(p, p) + \sum_{l_s l'_s} \tilde{\mathcal{C}}_{l'_p l'_s}(p, w) \Gamma_{l_s l'_s}^{-1} \Xi_{l'_s l_p} \right] \quad (9)$$

$$\text{where } \tilde{\mathcal{C}}_{l'_p l'_s}(p, w) \equiv \sum_{l_w} \mathcal{C}_{l'_p l_w}(p, w) \lambda_{l_w}^{1/2} T_{l_w l_s} \equiv \sum_{l_w} \bar{\mathcal{C}}_{l'_p l_w}(p, w) T_{l_w l_s}. \quad (10)$$

The vacuum energy can be then written as,

$$\frac{1}{2\pi^2} \delta W_V^{pp} = \sum_{l'_p l_p} \mathcal{B}_{l'_p}^p \mathcal{B}_{l_p}^{p*} \left[ \mathcal{C}_{l'_p l_p}(p, p) + \sum_{l_s l'_s} \tilde{\mathcal{C}}_{l'_p l'_s}(p, w) \Gamma_{l_s l'_s}^{-1} \Xi_{l'_s l_p} \right] \quad (11)$$

Eq. (9) together with Eq. (3) and Eq. (11) when coupled with appropriate stability codes such as NOVA, MARS, or DCON fully describe the feedback mechanism against external MHD modes. A special case where only Eq. (11) is required is described in the next section.

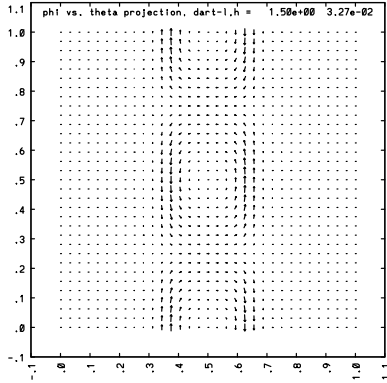


Figure 1: The Feedback Coil Current.

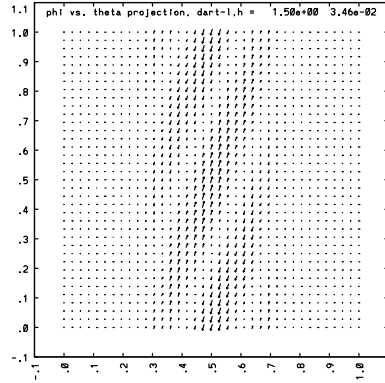


Figure 2: The Induced Current on the Resistive Shell.

## 5. Limiting Values: Checks for Consistency, and Idealized Feedback

Studies with the modified GATO-VACUUM have shown that the plasma reduces the time response of the shell currents,  $\tau_w$ , from  $\sim 6$  ms for a very small plasma to  $\sim 3.5$  ms for a fully developed DIII-D plasma. The induced surface current pattern, Fig. 2, on the shell is not significantly modified by the finite resistivity. Seven pairs of eigenmodes,  $\psi_l^w$ , are sufficient to accurately reproduce this pattern. This is to be compared with the results of [11, 12] and the lumped circuit parameter approach of [10]. In the limits,  $\gamma \hat{\tau} \rightarrow \infty$  and  $\gamma \hat{\tau} \rightarrow 0$ , the code accurately reproduces the perfectly conducting shell and no-wall results.

In a special situation, in which the plasma is surrounded by a resistive shell and a network of ‘(intelligent) flux conserving coils with  $\int \psi^w ds = 0$ ’ the feedback problem is still treatable by ideal MHD. We use a restricted set of  $\psi_l^w$  to correspond to the exclusion of magnetic flux through varying poloidal segments of the DIII-D vessel. This would indirectly simulate the effect of the sensor-feedback system while keeping the self-adjoint property of the system and we can ignore the terms involving the coil currents  $I_s$  in Eq. (11).  $\delta W_V$  depends on the coverage

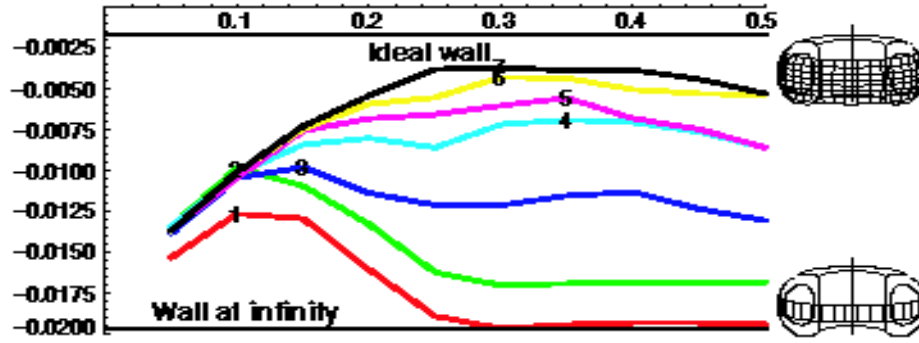


Figure 3:  $\delta W_V$  vs fractional length of poloidal coverage.

and the number of coil segments,  $n_s$ . The result of a GATO-VACUUM study is summarized in Fig. 3. The curves there are labeled by the number  $n_s$  of segments which are all of equal lengths.

The figure shows that (a) poloidal coverage of the existing feedback coils is close to being optimum when only one segment of the resistive shell is used for feedback stabilization; with feedback, the shell can be made to be 40% as effective as the ideal shell, (b) increasing the number of segments to 6 or 7 and increasing the poloidal coverage to 30% of the total circumference can make the resistive shell up to 90% as effective as an ideal shell, (c) in the present study and for the chosen equilibrium, mode deformation due to feedback was not significant. The optimum effectiveness defined by  $E_{\text{ff}} = (\delta W_R - \delta W_{\eta=\infty}) / (\delta W_{\eta=0} - \delta W_{\eta=\infty})$ , and coverage vs. number of segments  $n_s$  is tabulated in Fig. 4. Here,  $\delta W_R = \delta W_p + \delta W_V$ .

$n_s$	Total Coverage	$E_{\text{ff}}$
1	0.129	0.414
2	0.120	0.548
3	0.125	0.564
4	0.346	0.663
5	0.327	0.810
6	0.330	0.863
7	0.280	0.907

Figure 4: Dependence of optimum total poloidal length and effectiveness on  $n_s$ .

## References

- [1] M. Okabayashi, et al., *Nucl. Fusion* **36**, (1996) 1167.
- [2] T. Ivers, et al., *Phys. Plasmas* **3**, (1996) 1926.
- [3] E. J. Strait, T. S. Taylor, A. D. Turnbull, et al., *Phys. Rev. Lett.* **74**, (1995) 2483.
- [4] A. A. Garofalo, et al., *Phys. Plasmas* **6**, (1999) 1893.
- [5] P. Martin, et al., *Phys. Plasmas* **7**, (2000) 1984.
- [6] M. S. Chu, J. M. Greene, T. H. Jensen, et al., *Phys. Plasmas* **2**, (1995) 2236.
- [7] M. S. Chance, *Phys. Plasmas* **4**, (1997) 2161.
- [8] M. Okabayashi, et al., *26th EPS Conference on Controlled Fusion and Plasma Physics*, June, 1999.
- [9] A. H. Boozer, *Phys. Plasmas* **5**, (1998) 3350.
- [10] M. Okabayashi, N. Pomphrey and R. Hatcher, *Nuclear Fusion* **38**, (1998) 1607.
- [11] R. Fitzpatrick and T. Jensen, *Phys. Plasmas* **3**, (1996) 2641.
- [12] Y. Q. Liu and A. Bondeson, *Phys. Rev. Lett.* **84**, (2000) 907.